Development of new three-component BNP-inhibitor for carbon steel in 0.5 mol·dm^{-3} HCl solution. Thermodynamic, adsorption and electrochemical studies

T. Seilova, Z. Kunasheva, R. Kubasheva and N. Akatyev*

M. Utemisov West Kazakhstan university, Nazarbayev av. 162, Uralsk, Kazakhstan
**E-mail: nikolay.akatyev@wku.edu.kz*

Abstract

In this work, the development and investigation of a new *in situ* synthesised BNP-inhibitor based on boric acid (H_3BO_3), 1,4-phenylenediamine, and trisodium orthophosphate (Na_3PO_4) as an effective corrosion inhibitor for carbon steel were reported. The corrosion inhibition properties of the developed BNP-inhibitor were studied using the weight loss assay and electrochemical measurement. It was found that at the components molar ratio of 3:2:1 ($\times 10^{-3}$ mol·dm^{-3}) developed inhibitor demonstrates inhibition efficiency up to 93.2% in 0.5 mol·dm^{-3} HCl solution. Temperature, inhibitor concentration, molar ratio, and nature of the components strongly affect the degree of metal protection. The Langmuir adsorption model turned out to be the most suitable to describe the BNP-inhibitor adsorption mechanism. The free Gibbs energy change corresponds to spontaneous and physical nature of the inhibitor adsorption. Replacing the inhibitor components with similar counterparts does not lead to an increase in protective efficiency. Electrochemical results showed high efficiency of the BNP-inhibitor and are in excellent agreement with gravimetric data.

Received: November 27, 2024. Published: June 14, 2024 doi: 10.17675/2305-6894-2024-13-2-33

Keywords: *BNP-inhibitor, corrosion, adsorption, carbon steel, inhibition, metal protection, corrosion rate.*

1. Introduction

In the 21st century, corrosion remains one of the most important problems in industry and technology. Despite significant advances in corrosion science, corrosion damage can only be slowed down by various methods [1]. Modification of corrosion media by the addition of corrosion inhibitors is one of the low-cost, efficient, and economical anti-corrosion method [2].

Corrosion inhibitors can be subdivided into natural and synthetic [3]. A wide range of compounds containing sulphur [4], nitrogen [5], phosphorus [6], boron [7], and other heteroatoms are successfully used to protect different metals against corrosion in liquid and gaseous environments. Nevertheless, the search for alternatives that would replace toxic and expensive corrosion inhibitors that in some instances require rigorous process of synthesis is one of key problems in modern corrosion science [8]. The use of acid solutions in

production very often involves their operating at high temperatures, which requires the development of inhibitors with specific properties [9].

The most eco-friendly method for achieving the high anticorrosion characteristics of toxic inhibitors is through the gains vided by nontoxic corrosion inhibitors synergies. The idea of anticorrosive synergies is not a new concept but one that still holds a lot promise for advancing the performance of corrosion inhibitors [10]. Obviously, that such type of inhibitors must be multi-component and contain at least two compounds of different nature that should be easily synthesized, low-cost, available and non-toxic. Furthermore, these substances must preferably have low molecular weight, will make them more convenient for industrial applications. Low molecular weight components have better adsorb onto the metal surface, that in turn, leading to improve the properties of the protective coverage.

Inorganic inhibitors, such as chromates, phosphates, molybdates, and silicates, have been used to protect metals and alloys from corrosion in various industries [11]. Boron compounds are suitable as additives to lubricants [12], flame retardants, antioxidants, and corrosion inhibitors [13, 14]. Boric acid, the most available boron compound, can be used in combination with other corrosion inhibitors to enhance protective efficiency. Research has shown that the addition of boric acid to certain electrolytes can significantly increase the wear resistance of coatings and reduce the coefficient of friction, making it an effective corrosion inhibitor [15]. Furthermore, the study on the protective efficiency of water-soluble corrosion inhibitors found that boric acid combined with triethanolamine, slowed the anode reaction and decreased the corrosion rate of steel electrodes, demonstrating its potential as a corrosion inhibitor in combination with other compounds [16]. The inhibition efficiency of borates has been demonstrated to be over 98% after 30 days of immersion in simulated recirculating water, indicating their strong protective capability [17]. Elbadaoui *et al*. prepared and tested a new family of borated glasses against the corrosion of carbon steel in an acidic medium by electrochemical means. The developed system acts primarily as an anodic inhibitor with an efficiency of 95% [18]. Boulifi *et al*. demonstrated high protective efficiency of similar compositions [19]. 4-Carboxyphenylboronic acid (CPBA) has been found by Nam *et al*. to be an efficient carbon dioxide (CO_2) corrosion inhibitor for steel in aqueous media [20]. Boron-coordinated compounds with polyols were also found as good corrosion inhibitors [21]. The inhibition characteristics of sodium sorbitol borate and sodium mannitol borate on steel corrosion in aqueous media were investigated computationally by Gece [22]. These studies provide insights into the potential of boric acid as a possible component of mixed corrosion inhibitors, which in combination with other components can synergistically improve their anticorrosive properties to provide effective metal protection.

Organic amines are also widely used for metal protection against corrosion. Five and six-membered nitrogen-containing compounds with simple and complex ring systems are widely used in the field of protection of ferrous and nonferrous metals from corrosion damage in acidic solutions [23, 24]. Among nitrogen-containing inhibitors, phenylenediamines are known as components of anticorrosion polymer coatings [25, 26]. Croes *et al*. used the three isomers of phenylenediamine as crosslinking agents for epoxide-

decorated silica colloids. The resulting materials have demonstrated corrosion protection for aluminium alloys in corrosive environments [27]. Vasni and Patel have investigated the inhibitor effect of 1,2-phenylenediamine on the corrosion of brass in nitric acid solution. Inhibitor efficiency up to 97% was found in 0.1 M HNO_3 with 20 mM inhibitor concentration [28].

Phosphorus compounds have a long history of being used as important components of corrosion inhibitors [29]. Organic and inorganic phosphates both demonstrate corrosion inhibition properties, but their mechanisms and effectiveness can vary.

Inorganic phosphates are the most widespread inorganic components in anticorrosion compositions produced in large quantities in industry. They are well known as low-cost, non-toxic [30], non-oxidizing, and environmentally-friendly anodic inhibitors and as a great alternative to hazardous chromates [31]. On the other hand, inorganic phosphates, such as soluble phosphates like sodium monofluorophosphate (MFP), disodium hydrogen phosphate (DHP), and trisodium phosphate (TSP), have been found to promote ferrous phosphate precipitation, forming a protective barrier layer that hinders corrosion, making them anodic corrosion inhibitors [32]. However, it is important to note that the effectiveness of inorganic phosphates as corrosion inhibitors may vary depending on the specific application and environmental conditions. Additionally, the use of inorganic phosphates alone may not provide sufficient protection against corrosion in certain scenarios, as evidenced by the need for synergistic multi-component inhibitor formulations to enhance their effectiveness [33]. Based on the available sources, today there are no specific cost-effective alternatives to inorganic phosphates for corrosion inhibition mentioned.

In the case of iron corrosion in acidic solutions, research indicates that organic phosphates, such as monoalkyl phosphate esters, can act as mixed-type corrosion inhibitors with a dominant cathodic effect, with different chain lengths affecting their inhibition efficiency [34]. Due to the versatile molecular structures, phosphorus-based polymers are an important class of chemical inhibitors commonly adopted in oilfield operations [35]. Nevertheless, organophosphorus compounds very often exhibit bio-toxic properties, therefore traditional organophosphorus corrosion inhibitors are a significant concern due to their potential negative environmental and human health impacts [36]. While organophosphorus corrosion inhibitors may offer effective protection against corrosion [37], their toxicity [38] necessitates of the development of alternative, less toxic anticorrosion compositions.

Protective compositions based on two components are broadly known as well. Compositions obtained from boric acid and ethanolamines are widely used to protect carbon and mild steel in different corrosion media. They are water-soluble and can be easily synthesised from different ratios of components. Levashova synthesised low-cost, non-hazardous protective composition based on boric acid and amines with inhibitor efficiency of up to 93% [39]. The effect of pigment particle surface treatment with conductive polymers such as polyaniline phosphate on the corrosion-inhibiting properties of organic paints was investigated by Kalendová *et al.* [40]. High-performance anti-corrosive powder coatings

based on phosphate pigments containing poly(*o*-aminophenol) were developed by Abd El-Ghaffar *et al*. The obtained compositions showed high anti-corrosive properties for steel protection [41]. A similar system based on boron phosphate and poly(*p*-phenylenediamine) was developed and used as a coating for steel. However, synthesis of this system required several steps, including pyrolysis and polymerisation. The composition was tested as a corrosion inhibitor in artificial seawater within paints based on epoxy resin [42].

As can be seen, combining the beneficial properties of all the types of inhibitors considered will make it possible to develop an effective, cheap and environmentally friendly method of protecting metals from corrosion damage. As potential candidates for the development of an inhibitor based on a synergistic effect, we can consider the most available compounds of nitrogen, boron and phosphorus that correspond to the specified characteristics. Therefore, the main goal of our research is to develop an effective corrosion inhibitor that contains boron (B), nitrogen (N), and phosphorus (P) components, *i.e*., BNP-inhibitor. For this purpose, boric acid (H_3BO_3), phenylenediamines (PDA's), and sodium phosphates were chosen. Combining the three components could result in a simple, effective corrosion inhibitor that can be easily produced by dissolution of the required amounts of the available low-cost components in corrosion medium.

2. Materials and Methods

2.1. Corrosion media and inhibitor preparation

All reagents of analytical grade were purchased in Sigma Aldrich, Merck, and Alfa Aesar and used without any further purification. Corrosion media were prepared by dissolution of the required amount of acid or salt in double distilled water. Tap water with characteristics of pH 7.17±0.29, electrical conductivity 1058±72 μS (534±31 mg·dm^{-3} NaCl), solid content 489±27 mg·dm^{-3}, total hardness 6.13±0.17 mmol·dm^{-3}, chlorides 236±28 mg·dm^{-3} and Fe^{3+} 0.19±0.08 mg·dm^{-3} was used directly from the tap. Investigated BNP-compositions were prepared by reagent dissolution in corrosion media. All weight measurements were performed using Ohaus Adventurer Pro AV264 analytical balance with an accuracy of ±0.1 mg.

2.2. Specimens preparation

Carbon steel specimens used in this investigation with exposed areas of 2.5×3.5×0.3 cm with compositions of (wt.%) 97.8 – Fe; 0.22 – C; 0.65 – Mn; 0.30 – Si; 0.04 – P; 0.05 – S; 0.30 – Cr; 0.30 – Ni; 0.30 – Cu; 0.01 – N; 0.08 – As; were obtained from industry. Before the experiment, coupons were polished until a mirror by emery sheets with 250, 300, 800, and 1200 grit numbers. Then the abraded specimens were cleaned from dust, grease, and oxides by washing in running water, double distilled water, ethanol, acetone, dried, and weighed.

2.3. Weight loss (gravimetric) method

Weight loss experiments were performed to evaluate the corrosion rate (*CR*), inhibition efficiency (*IE*), and degree of surface coverage (θ). For investigation, each coupon was immersed in an open-to-air 100 mL beaker containing 75 mL of corrosion medium at a room temperature of 18 h. Following the designated immersion period, coupons were taken out of the beaker, and the corrosion products were eliminated by washing each coupon in a solution comprising 50% NaOH and 100 g of zinc dust [43]. Then, coupons were again washed in running water, double distilled water, rinsed in ethanol, acetone and dried in air before reweighting. All measurements of weight were performed using Ohaus Adventurer Pro AV264 analytical balance with an accuracy of ±0.1 mg.

The corrosion rate (*CR* $g \cdot m^{-2} \cdot h^{-1}$), inhibition efficiency (*IE*%), and degree of surface coverage (θ) were calculated according to Equations (1–3) respectively:

$$CR\,(g \cdot m^{-2} \cdot h^{-1}) = \frac{\Delta m}{S\tau} \tag{1}$$

$$IE(\%) = \frac{CR_0 - CR_i}{CR_0} \cdot 100 \tag{2}$$

$$\theta = \frac{IE}{100} \tag{3}$$

where Δm is the weight loss of steel coupon (g) after the period of immersion (h), CR_0 is the corrosion rate of carbon steel without inhibitor, and CR_i is the corrosion rate of carbon steel in the presence of the inhibitor. The degree of surface coverage of the inhibitor was estimated on the assumption of the blocking mechanism of action of the inhibitor.

2.4. Electrochemical measurement

The polarisation studies were carried out in 0.5 $mol \cdot dm^{-3}$ HCl in the absence and presence of different concentrations of BNP-inhibitor. Steel coupons after pre-treatment as for weight loss assay were used for the electrochemical experiment. The electrochemical testing was performed using the Autolab PGSTAT 101 Metrohm potentiostat/galvanostat device equipped with NOVA 2.1.6 software. In the method of potentiodynamic polarisation three-electrode setup was used: Ag/AgCl (3 M KCl) as the reference electrode, the platinum as counter electrode, and steel coupon connected with a specimen alligator clamp to serve as the working electrode. The electrochemical cell was of 100 mL of 0.5 $mol \cdot dm^{-3}$ HCl in the presence and absence of different concentrations of BNP-inhibitor in a glass beaker at room temperature. The working electrode, with a 1.00 cm^2 exposed area was stabilised at open circuit potential (OCP) testing. The linear polarisation measurements were performed immediately after the OCP by running a Linear Sweep Voltammetry (LSV) staircase and corrosion rate analysis. The potentiodynamic scan was carried out from –0.50 to +0.50 V at

a scan rate of 0.001 V/s and a step voltage of 0.001 V. The corrosion potential (E_{corr}) and corrosion current density (i_{corr}) were determined from the Tafel polarisation curves.

The polarisation resistance (R_p) was calculated using Equation (4):

$$R_p = \frac{\beta_a \beta_c}{2.303 i_{corr} (\beta_a + \beta_c)} \quad (4)$$

where β_a and β_c denote the slopes of the anodic and cathodic Tafel lines, respectively.

The inhibition efficiency through the polarization resistance (IE_R%) was calculated using the following Equation (5):

$$IE_R(\%) = \frac{R_p^{inh} - R_p^0}{R_p^{inh}} \cdot 100 \quad (5)$$

where R_p^{inh} and R_p^0 are the polarization resistance in the presence and absence of inhibitor, Ω.

3. Results and Discussion

3.1. Development of optimal inhibitor composition and choice of corrosion medium by weight loss measurement

Our investigation starts from the screening of the protective efficiency of the three-component compositions based on boric acid, phenylenediamines, and sodium phosphates at the molar ratio of 1:3:3 at concentration $x \cdot 10^{-3}$ mol·dm^{-3}. Screening was carried out in the 18 acidic and neutral corrosion media includes inorganic and organic acids (HCl, H_2SO_4, HNO_3, H_3PO_4, CH_3COOH) in different concentrations (0.1, 0.5, 1.0 mol·dm^{-3}), tap water, 3% NaCl and the model environment recommended by the National Association of Corrosion Engineers of USA (NACE) contains 5.0 g·dm^{-3} NaCl and 0.25 g·dm^{-3} CH_3COOH [44]. The results of the screening are depicted in Table 1.

Results show that among 162 systems tested in the experiment 73 (45%) demonstrated negative results. Almost all of them appeared in the least aggressive environments containing sodium chloride and acetic acid, both together and separately, and in tap water. In other cases, inhibition efficiency ranged from 0.3 to 79.2%. The highest inhibition efficiency was determined for the composition containing H_3BO_3 + 1,4-phenylenediamine + Na_3PO_4 in 0.5 mol·dm^{-3} HCl (79.2%). Therefore, this BNP-composition and corrosion media were chosen as the next step of our investigation.

In the next step of our research, we were going to modify the most effective system to increase its protective efficiency. BNP-inhibitor was tested in 0.5 mol·dm^{-3} HCl medium in accordance with the components ratio. The inhibition efficiency of the compositions based on H_3BO_3, 1,4-phenylenediamine, and Na_3PO_4 with different components ratios are given in Table 2.

Table 1. The inhibition efficiency (*IE*%) of compositions based on H_3BO_3 ($1 \cdot 10^{-3}$ mol·dm^{-3}), phenylenediamines ($3 \cdot 10^{-3}$ mol·dm^{-3}) and sodium orthophosphates ($3 \cdot 10^{-3}$ mol·dm^{-3}) against corrosion of carbon steel in different corrosion media at room temperature.

Corrosion media	H_3BO_3 + 1,2-phenylendiamine			H_3BO_3 + 1,3-phenylendiamine			H_3BO_3 + 1,4-phenylendiamine		
	Na_3PO_4	Na_2HPO_4	NaH_2PO_4	Na_3PO_4	Na_2HPO_4	NaH_2PO_4	Na_3PO_4	Na_2HPO_4	NaH_2PO_4
Tap water	11.7	N/R	N/R	N/R	N/R	N/R	N/R	N/R	N/R
HCl 0.1 M	40.7	47.3	53.1	55.0	59.0	64.1	69.3	70.7	75.1
HCl 0.5 M	N/R	40.7	16.6	35.3	55.5	40.7	79.2	70.2	64.8
HCl 1 M	N/R	34.5	N/R	N/R	53.7	13.4	N/R	52.8	49.0
H_2SO_4 0.1 M	2.7	34.3	7.5	38.6	40.2	24.3	74.4	45.9	41.0
H_2SO_4 0.5 M	N/R	12.2	N/R	9.0	22.0	1.2	37.2	31.7	14.3
H_2SO_4 1 M	N/R	8.5	N/R	N/R	20.2	1.1	35.0	31.9	15.8
HNO_3 0.1 M	0.3	8.4	21.2	29.5	10.4	22.0	38.2	12.4	22.8
HNO_3 0.5 M	27.1	29.3	31.2	19.3	20.0	16.5	31.8	10.7	3.9
HNO_3 1 M	19.0	18.2	15.2	N/R	11.4	9.6	N/R	4.6	1.7
H_3PO_4 0.1 M	24.6	30.6	70.0	32.7	43.1	65.4	40.7	55.6	60.7
H_3PO_4 0.5 M	N/R	22.2	N/R	14.8	40.9	22.1	47.8	50.8	49.0
H_3PO_4 1 M	N/R	20.7	N/R	13.2	36.5	19.9	66.0	61.1	47.7
CH_3COOH 0.1 M	N/R	N/R	N/R	N/R	N/R	N/R	N/R	N/R	N/R
CH_3COOH 0.5 M	9.3	46.9	N/R	N/R	N/R	N/R	N/R	N/R	N/R
CH_3COOH 1 M	N/R	25.8	24.7	N/R	N/R	9.8	N/R	N/R	N/R
NACE media	N/R	N/R	N/R	N/R	N/R	N/R	N/R	N/R	N/R
NaCl 3%	N/R	N/R	N/R	N/R	N/R	N/R	N/R	N/R	N/R

N/R – negative result.

Table 2. The inhibition efficiency (*IE*%) of BNP-compositions based on H_3BO_3, 1,4-phenylenediamine (1,4-PDA), and Na_3PO_4 against corrosion of carbon steel in 0.5 mol·dm^{-3} HCl solution depending on the component ratio.

Entry	Components concentration, ×·10^{-3} mol·dm^{-3}			Corrosion rate g·m^{-2}·h^{-1}	*IE*%
	H_3BO_3	1,4-PDA	Na_3PO_4		
1	–	–	–	7.63	–
2	1	1	1	2.19	71.3
3	1	3	1	2.06	73.0
4	1	1	3	1.68	78.0
5*	1	3	3	1.58	79.2
6	3	3	3	1.47	80.7
7	1	2	2	1.32	82.7
8	1	2	3	2.58	66.2
9	3	1	3	4.30	43.6
10	3	2	1	0.52	93.2
11	3	2	–	2.07	72.8
12	–	2	1	2.06	72.9
13	3	–	1	12.99	N/R
14	3	–	–	15.54	N/R
15	–	2	–	3.07	59.7
16	–	–	1	15.44	N/R

*data from Table 1. N/R – negative result.

Table 2 shows that the most effective BNP-inhibitor contains $3\cdot10^{-3}$ mol·dm^{-3} of H_3BO_3, $2\cdot10^{-3}$ mol·dm^{-3} of 1,4-phenylenediamine and $1\cdot10^{-3}$ mol·dm^{-3} of Na_3PO_4 (molar ratio 3:2:1). The composition has demonstrated inhibition efficiency of 93.2% (Entry 10). Other ratios of the components do not give high protection efficiency in the given medium and inhibition efficiency values range from 43.6 to 82.7% (Entries 2–9). Removing one of the components leads to a significant decrease in the inhibition efficiency up to negative values (Entries 11–3). Individual components did not demonstrate inhibition efficiency in the given medium. Negative results were obtained with only boric acid and sodium orthophosphate (Entries 14, 16). Pure 1,4-phenylendiamine showed an inhibition efficiency of 59.7% (Entry 15).

Based on the obtained results, we assumed that the replacement of components could lead to an improvement in the protective efficiency of the developed inhibitor. Therefore, we change boric acid to sodium tetraborate and phenylboronic acid, 1,4-phenylenediamine to

isomeric diamines, and 1,1′-biphenyl-4,4′-diamine (benzidine) and sodium orthophosphate to potassium salts and corresponding diphosphates. The ratio of components remains the same. Experimental results are given in Table 3.

Table 3. The inhibition efficiency (*IE*%) of BNP-compositions against corrosion of carbon steel in 0.5 mol·dm^{-3} HCl in accordance with the components' nature.

Entry	B-component $3\cdot10^{-3}$ mol·dm^{-3}	N-component $2\cdot10^{-3}$ mol·dm^{-3}	P-component $1\cdot10^{-3}$ mol·dm^{-3}	Corrosion rate g·m^{-2}·h^{-1}	*IE*%
1*	H_3BO_3	1,4-PDA	Na_3PO_4	0.52	93.2
2	H_3BO_3	1,3-PDA	Na_3PO_4	2.06	73.0
3	H_3BO_3	1,2-PDA	Na_3PO_4	7.33	3.8
4	H_3BO_3	1,1′-biphenyl-4,4′-diamine (benzidine)	Na_3PO_4	4.26	44.1
5	H_3BO_3	1,4-PDA	Na_2HPO_4	3.02	60.4
6	H_3BO_3	1,4-PDA	NaH_2PO_4	1.95	74.4
7	H_3BO_3	1,4-PDA	K_3PO_4	3.57	53.2
8	$Na_2B_4O_7$	1,4-PDA	Na_3PO_4	3.57	53.2
9	H_3BO_3	1,4-PDA	$Na_4P_2O_7$	3.62	52.3
10	H_3BO_3	1,4-PDA	$K_4P_2O_7$	1.94	74.5
11	H_3BO_3	1,4-PDA·2 HCl	Na_3PO_4	1.41	81.5
12	$C_6H_5B(OH)_2$	1,4-PDA	Na_3PO_4	1.03	86.5

*data from Table 2 Entry 10.

As it can be seen from Table 3, replacing the inhibitor's components while preserving the components' molar ratio of 3:2:1 does not lead to an increase in inhibition efficiency. A change in any component led to a significant reduction of the protective properties. Therefore, inhibitor containing $3\cdot10^{-3}$ mol·dm^{-3} of H_3BO_3, $2\cdot10^{-3}$ mol·dm^{-3} of 1,4-phenylenediamine and $1\cdot10^{-3}$ mol·dm^{-3} of Na_3PO_4 (Entry 1) is the most effective to protect carbon steel in 0.5 mol·dm^{-3} HCl solution.

3.2 Effect of temperature and concentration

Additionally, the inhibitor that was developed underwent testing under different conditions of concentration and temperature. To achieve this, the temperature range was set from 303 to 353 K with a 10-degree interval. Total inhibitor concentration given as a sum of the molar concentration of the components and was ranged from 1.5 to $12\cdot10^{-3}$ mol·dm^{-3} corresponding to 0.14 to 1.13 g·dm^{-3}, respectively. The experiment was carried out for 2 h. Results of corrosion rate determination of carbon steel in 0.5 M HCl solution in the presence and absence of BNP-inhibitor at different temperatures and inhibitor concentrations are presented in Table 4.

Table 4. Corrosion rate (*CR*), inhibition efficiency (*IE*%), and degree of surface coverage (θ) of carbon steel at 2 h immersion in 0.5 mol·dm^{-3} HCl solution in the presence and absence of different concentrations of BNP-inhibitor at 303–353 K temperature range.

Inhibitor composition				**Temperature**								
H_3BO_3	**1,4-PDA**	**Na_3PO_4**	C_{BNP}	**303 K**			**313 K**			**323 K**		
×·10^{-3} mol·dm^{-3}			**g·dm^{-3}**	***CR*** **g·m^{-2}·h^{-1}**	***IE*** **%**	**θ**	***CR*** **g·m^{-2}·h^{-1}**	***IE*** **%**	**θ**	***CR*** **g·m^{-2}·h^{-1}**	***IE*** **%**	**θ**
0	0	0	0	15.20	–	–	25.72	–	–	35.70	–	–
0.75	0.5	0.25	0.14	4.55	70.07	0.7007	8.76	65.96	0.6596	13.90	61.06	0.6106
1.5	1	0.5	0.28	4.15	72.70	0.7270	7.86	69.44	0.6944	12.44	65.15	0.6515
3	2	1	0.57	3.29	78.36	0.7836	6.49	74.75	0.7475	11.34	68.23	0.6823
4.5	3	1.5	0.85	2.43	84.01	0.8401	5.88	77.14	0.7714	9.27	74.03	0.7403
6	4	2	1.13	1.09	92.83	0.9283	4.30	83.27	0.8327	8.11	77.27	0.7727
H_3BO_3	**1,4-PDA**	**Na_3PO_4**		**333 K**			**343 K**			**353 K**		
0	0	0	0	67.67	–	–	109.40	–	–	357.27	–	–
0.75	0.5	0.25	0.14	32.10	52.56	0.5256	59.70	45.43	0.4543	213.86	40.14	0.4014
1.5	1	0.5	0.28	26.59	60.70	0.6070	56.42	48.43	0.4843	191.00	46.54	0.4654
3	2	1	0.57	22.41	66.89	0.6689	47.49	56.59	0.5659	160.59	55.05	0.5505
4.5	3	1.5	0.85	20.20	70.16	0.7016	40.34	63.13	0.6313	149.05	58.28	0.5828
6	4	2	1.13	19.61	71.02	0.7102	35.53	67.52	0.6752	142.87	60.01	0.6001

The data in Table 4 shows that the rate of corrosion damage of metal increases with increasing temperature and decreasing inhibitor concentration. Increasing the inhibitor concentration leads to a significant increase in inhibitory efficiency and even at high temperatures can reach almost 70%. At not very high temperatures (up to 40°C), the developed inhibitor exhibits excellent protective ability (70–90%) relative to carbon steel even at low concentrations.

3.3. Activation energy calculations

To study the temperature effect, steel specimens were immersed for 2 h in corrosion media in the presence and absence of different concentrations of BNP-inhibitor and at 303–353 K temperature range with 10-degree intervals. The temperature was controlled by a water thermostat with an accuracy of ±0.1°.

The effect of temperature on the corrosion rate of carbon steel in 0.5 mol·dm^{-3} HCl solution in the presence and absence of the BNP-inhibitor was calculated using the Arrhenius equation [45]

$$\log\frac{CR_2}{CR_1} = \frac{E_a}{2.303R}\cdot\left(\frac{1}{T_1}-\frac{1}{T_2}\right) \tag{6}$$

where CR_1 and CR_2 are corrosion rates of carbon steel (g·m^{-2}·h^{-1}) at T_1 and T_2 respectively, E_a is the activation energy, and R is the universal gas constant (8.314 J·mol^{-1}·K^{-1}).

Enthalpy (ΔH*, kJ·mol^{-1}) and entropy (ΔS*, J·mol^{-1}·K^{-1}) of activation were obtained from the slope $-\Delta H/2.303R$ and intercept [$\log R/Nh + (\Delta S/2.303R)$] respectively from the plot of $\log CR/T$ *versus* $1/T$ in accordance with the following alternative form of Arrhenius equation [46]:

$$\log\frac{CR}{T} = \frac{-\Delta H}{2.303R}\left(\frac{1}{T}\right)+\left[\log\frac{R}{N_A h}+\left(\frac{\Delta S}{2.303R}\right)\right] \tag{7}$$

where h signifies Planck's constant, N_A – denotes Avogadro's number, CR is the corrosion rate, T represents thermodynamic temperature, R denotes the universal gas constant, ΔS is the entropy change, and ΔH signifies the enthalpy change.

Figure 1 shows the transition state plots for carbon steel in 0.5 mol·dm^{-3} HCl solution in the absence and presence of different concentrations of BNP-inhibitor for 2 h immersion time.

A graphical representation of $\log(CR/T)$ *versus* $1/T$ exhibits as straight lines. The slopes allow to estimate of enthalpy change and intercepts are appropriate to entropy change in accordance with Equation (7).

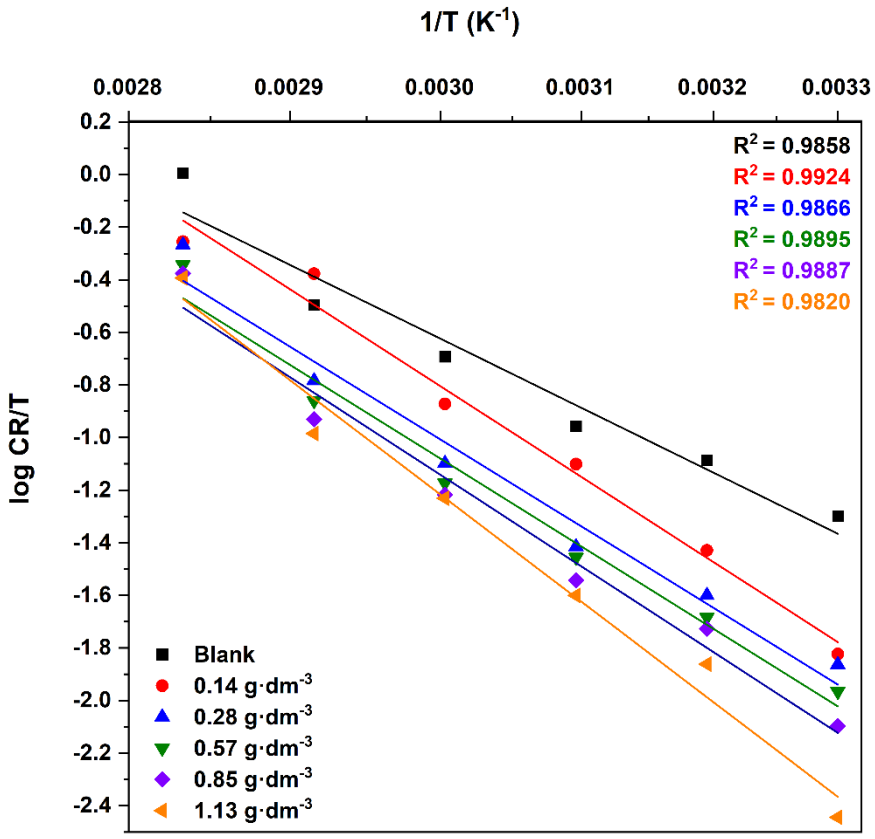

Figure 1. Transition state plots for carbon steel in 0.5 mol·dm^{-3} HCl solution in the absence and presence of different concentrations of BNP-inhibitor for 2 h immersion time.

The heat of adsorption (Q_{ads}) of BNP-inhibitor on the metal surface was obtained for the trend of surface coverage with temperature using the following Equation (8):

$$Q_{ads} = 2.303R\left(\log\frac{\theta_2}{1-\theta_2} - \log\frac{\theta_1}{1-\theta_1}\right)\cdot\left(\frac{T_1T_2}{T_2-T_1}\right) \quad (8)$$

The obtained values of activation energy (E_a), heat of adsorption (Q_{ads}), enthalpy (ΔH^*) and entropy (ΔS^*) of activation are listed in Table 5.

Negative enthalpy change values unequivocally signify that the adsorption of the BNP inhibitor on the carbon steel surface is exothermic. It was noted that as the inhibitor concentration increases, the enthalpy of activation decreases, signifying a more efficient sorption of the inhibitor.

The increase in entropy change values suggests a reduction in disorder during the formation stage of the activated complex from the inhibitor components, corresponding to the association process in the rate-limiting step [28]. This reduction occurs due to the replacement of water molecules during the adsorption process [29]. Consequently, the adsorption process becomes more effective with an increase in inhibitor concentration [30].

Table 5. Activation parameters of the dissolution of carbon steel in 0.5 mol·dm^{-3} HCl in the absence and presence of different concentrations of BNP-inhibitor for 2 h immersion time.

Inhibitor concentration ×·10^{-3} mol·dm^{-3}			g·dm^{-3}	E_a, kJ·mol^{-1}	Q_{ads}, kJ·mol^{-1}	ΔH^*, kJ·mol^{-1}	ΔS^*, J·mol^{-1}·K^{-1}
H_3BO_3	1,4-PDA	Na_3PO_4					
Blank				27.59	–	–4.68	–166.76
0.75	0.5	0.25	0.14	38.90	–17.81	–5.89	–155.48
1.5	1	0.5	0.28	38.66	–16.44	–5.88	–154.57
3	2	1	0.57	46.92	–27.01	–5.95	–152.92
4.5	3	1.5	0.85	38.31	–14.18	–6.19	–150.73
6	4	2	1.13	53.37	–32.07	–7.25	–145.02

It was found that the value of activation energy (E_a) in the presence of the inhibitor is greater than that of the without it. A higher value of the activation energy (E_a) of the process in an inhibitor's presence is attributed to physisorption [47]. However, the values of the activation energy are more significant than the values of the heat of adsorption. It indicates that the corrosion process involves the hydrogen gas evolution reaction [48].

3.4. Adsorption isotherms and thermodynamic parameters

Most organic inhibitors are adsorbed onto the metal surface by displacing water molecules and forming a barrier. The efficiency of the inhibitor depends on the stability of the chelate formed, which in turn depends on the type and nature of the inhibitor molecule [49].

Adsorption of an inhibitor to the metal surface may have a chemical, physical, or mixed nature. To describe the adsorption mechanism, the values of ΔG^0_{ads} must be determined. The ΔG^0_{ads} values up to –20 kJ·mol^{-1} indicate the electrostatic interaction between the metal surface and charged inhibitor molecules (physisorption). Values around –40 kJ·mol^{-1} are usually accepted as a threshold value between chemisorption and physisorption, or less indicate the chemical nature of sorption [50]. It occurs because of electrons transfer from the organic molecules to the metal surface with the formation of a coordination-type bond. To elucidate the BNP-inhibitor adsorption mechanism to the carbon steel surface the Langmuir, Freundlich, Temkin, and Flory–Huggins adsorption isotherm models were applied using the data of the corrosion rate (*CR*), degree of surface coverage (θ) for various inhibitor concentrations.

Langmuir adsorption isotherm was used in accordance with the following equation [51]:

$$\frac{C_{\text{inh}}}{\theta} = \frac{1}{K_{\text{ads}}} + C_{\text{inh}} \tag{9}$$

where θ is the degree of surface coverage, C_{inh} the concentration of the inhibitor and K_{ads} is the equilibrium constant of the adsorption-desorption process.

Logarithmic expression of Equation (9) yields to Equation (10):

$$\log\left(\frac{C_{\text{inh}}}{\theta}\right) = \log C_{\text{inh}} - \log K_{\text{ads}} \tag{10}$$

Plotting $\log(C/\theta)$ *versus* $\log C$ gave linear relationship where slope represents $\log K$. Langmuir adsorption isotherms for BNP-inhibitor are shown in Figure 2a. Parameters of Langmuir isotherms are presented in Table 6.

The Freundlich adsorption isotherm [52] is represented by the following Equation (11):

$$\log\theta = \log K_{\text{ads}} + n\log C_{\text{inh}} \tag{11}$$

A linear relationship between $\log\theta$ against $\log C$ is given in Figure 2b. The adsorption parameters obtained are also listed in Table 6.

For Temkin adsorption isotherm the degree of surface coverage (θ) is related to the logarithm of the inhibitor concentration in accordance with the following equation [53]:

$$\theta = \ln C_{\text{inh}} + K_{\text{ads}} \tag{12}$$

The slope of the line of the plot of θ against $\ln C$ depicted in Figure 2c gives the value of K_{ads}. The values of adsorption parameters obtained from the Temkin isotherms are given in Table 6.

The Flory–Huggins adsorption isotherm is given by equation [54]:

$$\log\frac{\theta}{C_{\text{inh}}} = b\log(1-\theta) + \log K_{\text{ads}} \tag{13}$$

where K denotes the adsorption-desorption constant. Corresponding linear plots are presented in Figure 2d. The values for Flory–Huggins adsorption parameters are listed in Table 6.

The relationship between free Gibbs energy and adsorption equilibrium constant is expressed by Equation (14).

$$\Delta G^0_{\text{ads}} = -RT\ln(55.5K_{\text{ads}}) \tag{14}$$

where ΔG^0_{ads} is the free Gibbs energy of adsorption, R is the universal gas constant (8.314 $\text{J}\cdot\text{K}^{-1}\cdot\text{mol}^{-1}$), T is the thermodynamic temperature of the system and 55.5 $\text{mol}\cdot\text{dm}^{-3}$ is the molar concentration of water.

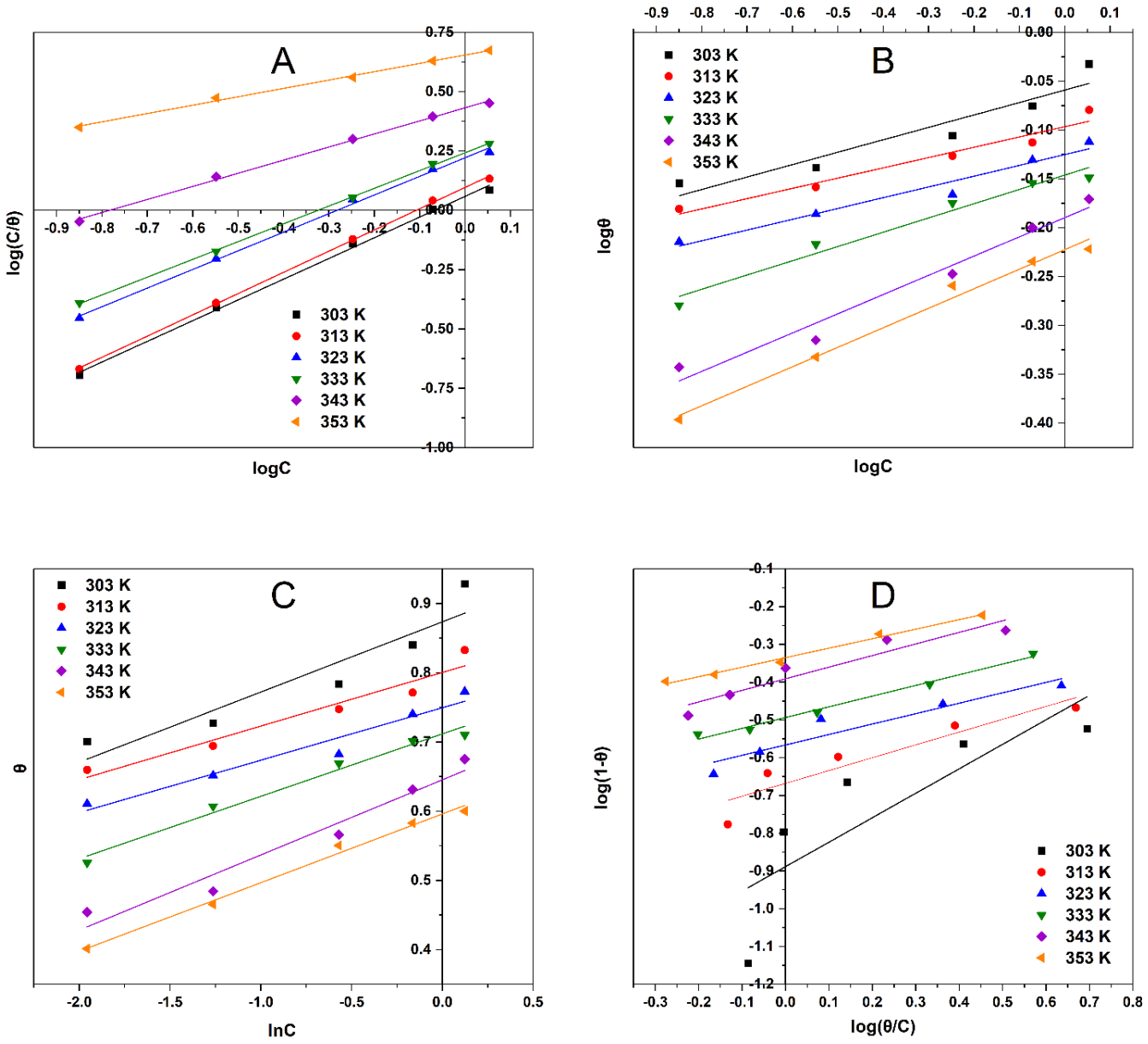

Figure 2. Adsorption isotherms for BNP-inhibitor on steel surface in 0.5 mol·dm^{-3} HCl at 303–353 K: a – Langmuir, b – Friendlich, c – Temkin, d – Flory–Huggins.

The obtained plots are almost linear with correlation coefficients (R^2) ranged from 0.6905 to 0.9997. Adsorption parameters obtained from isotherms are listed in Table 6.

Table 6. Parameters for adsorption of the BNP-inhibitor containing H_3BO_3 ($3 \cdot 10^{-3}$ mol·dm^{-3}), 1,4-PDA ($2 \cdot 10^{-3}$ mol·dm^{-3}) and Na_3PO_4 ($1 \cdot 10^{-3}$ mol·dm^{-3}) on steel surface in 0.5 10^{-3} mol·dm^{-3} HCl solution.

Isotherm	Temperature	R^2	Slope	Intercept	K_{ads}	ΔG_{ads}, kJ·mol^{-1}
Langmuir	303 K	0.9977	0.8728	0.0591	16.9291	–17.25
	313 K	0.9994	0.8948	0.0965	10.3584	–16.54
	323 K	0.9976	0.7845	0.2216	4.5118	–14.83
	333 K	0.9997	0.7487	0.3426	2.9188	–14.09
	343 K	0.9978	0.5520	0.4322	2.3138	–13.85
	353 K	0.9964	0.3522	0.6545	1.5278	–13.03
Freundlich	303 K	0.9023	0.1272	–0.0591	0.8728	–9.78
	313 K	0.9577	0.1052	–0.0965	0.8008	–9.88
	323 K	0.9612	0.1103	–0.1251	0.7497	–10.01
	333 K	0.9709	0.1461	–0.1461	0.7143	–10.19
	343 K	0.9690	0.1968	–0.1896	0.6462	–10.21
	353 K	0.9870	0.1998	–0.2223	0.5994	–10.29
Temkin	303 K	0.8777	0.1014	0.8736	0.8736	–9.78
	313 K	0.9428	0.0775	0.8004	0.8004	–9.87
	323 K	0.9493	0.0756	0.7494	0.7494	–10.01
	333 K	0.9816	0.0902	0.7118	0.7118	–10.18
	343 K	0.9540	0.1086	0.6454	0.6454	–10.21
	353 K	0.9920	0.0992	0.5961	0.5961	–10.27
Flory–Huggins	303 K	0.6905	0.6482	–0.8885	0.1293	–4.96
	313 K	0.8660	0.3397	–0.6679	0.2148	–6.45
	323 K	0.9025	0.2762	–0.5661	0.2716	–7.29
	333 K	0.9878	0.2839	–0.4937	0.3209	–7.97
	343 K	0.9061	0.3073	–0.3908	0.4066	–8.89
	353 K	0.9902	0.2516	–0.3350	0.4624	–9.53

The experimental data indicates that the Langmuir adsorption model is the most appropriate for describing the adsorption behaviour of the BNP-inhibitor under all tested temperature conditions. Langmuir isotherms manifest as straight lines, clearly indicating a good fit between the data and the plotted isotherm. This observation suggests that the adsorption of the inhibitor takes place as a monolayer, involving a well-defined number of

uniform and energetically identical adsorption sites [38]. The values of the adsorption equilibrium constant (K_{ads}) obtained from the intercept of the adsorption isotherms are related to the free Gibbs energy (ΔG^0_{ads}) of adsorption according to Equation (14). The results show that obtained Gibbs free energy values are negative and less than the threshold value required for chemical adsorption. It is generally known that free Gibbs energy values greater than –40 kJ·mol^{-1} clearly indicate that adsorption is physical [55]. Thus, the adsorption of BNP-inhibitor in carbon steel surface is a spontaneous process that occurs according to the mechanism of physical adsorption as electrostatic interactions between the negatively charged inhibitor molecules and the positively charged metallic surface [56]. Moreover, the application of Langmuir isotherm to the adsorption of BNP-inhibitor indicates the absence of interaction between the molecules adsorbed at the metal surface [57].

3.5. Potentiodynamic polarization measurements

The results of the electrochemical experiment are given in Figure 3.

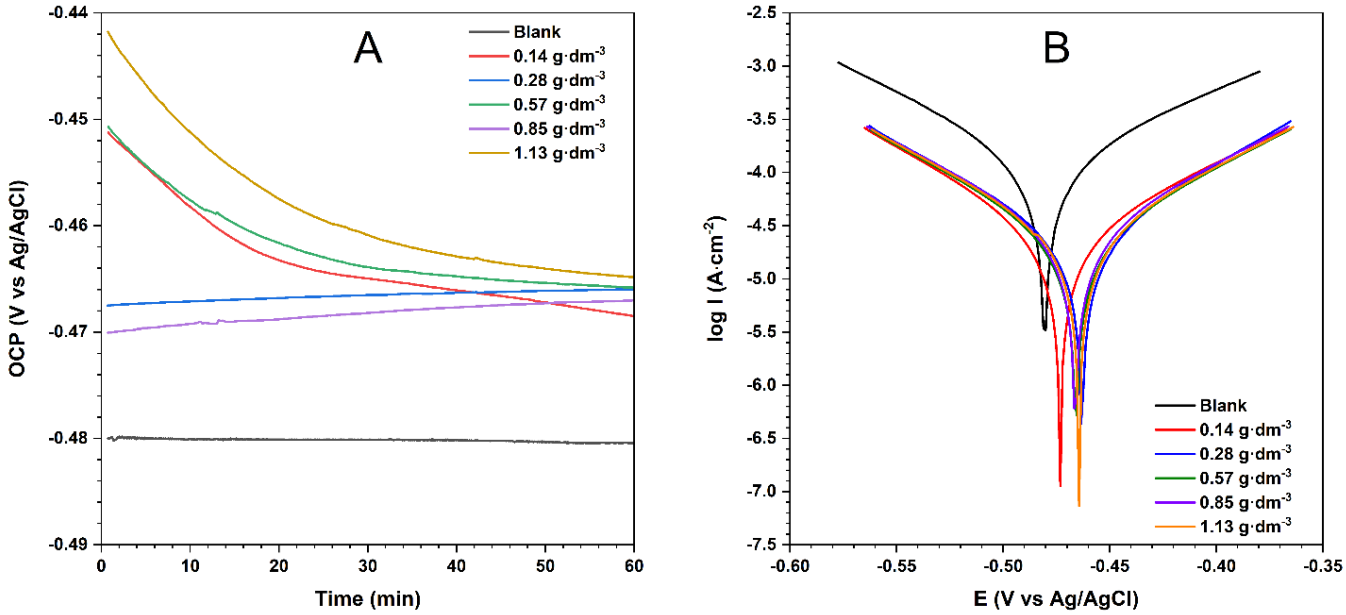

Figure 3. Open circuit potential (A) and Tafel polarisation curves (B) for BNP-inhibitor in 0.5 mol·dm^{-3} HCl solution at different concentrations.

The inhibition efficiency and polarization resistance parameters are listed in Table 7.

With the increase in inhibitor concentration, a decline in corrosion potential (E_{corr}), corrosion current density (i_{corr}), and a corresponding increase in polarisation resistance (R_p) were observed. This indicates that the formation of a protective film on the metal surface in the presence of inhibitor, leads to a decrease in surface area available for electrode reactions [59], and, thereby to a decrease in the corrosion rate and an increase in the degree of inhibition efficiency.

Table 7. Potentiodynamic polarisation parameters for the corrosion of mild steel in 0.5 mol·dm^{-3} HCl in the absence and presence of different concentrations of BNP-inhibitor.

C_{BNP}, g·dm^{-3}	–OCP, mV	$-E_{corr}$ (mV *vs.* Ag/AgCl)	i_{corr}, A·cm^{-2}	R_p, Ω	IE_R, %
Blank	480.4	480.6	$1.13\cdot10^{-4}$	210.32	–
0.14	468.3	473.3	$2.48\cdot10^{-5}$	906.74	76.80
0.28	465.9	463.1	$2.33\cdot10^{-5}$	913.81	76.98
0.57	465.7	465.8	$2.30\cdot10^{-5}$	930.19	77.39
0.85	467.1	466.2	$2.13\cdot10^{-5}$	937.10	77.56
1.13	464.7	464.4	$2.12\cdot10^{-5}$	962.83	78.16

3.6. Surface analysis

The protective efficiency of the BNP-inhibitor on corrosion was also studied by the micro images of corroded steel surfaces. Microscope images of carbon steel specimens before and after the immersion in 0.5 mol·dm^{-3} HCl solution in the absence and presence of the most effective BNP-inhibitor are depicted in Figure 4.

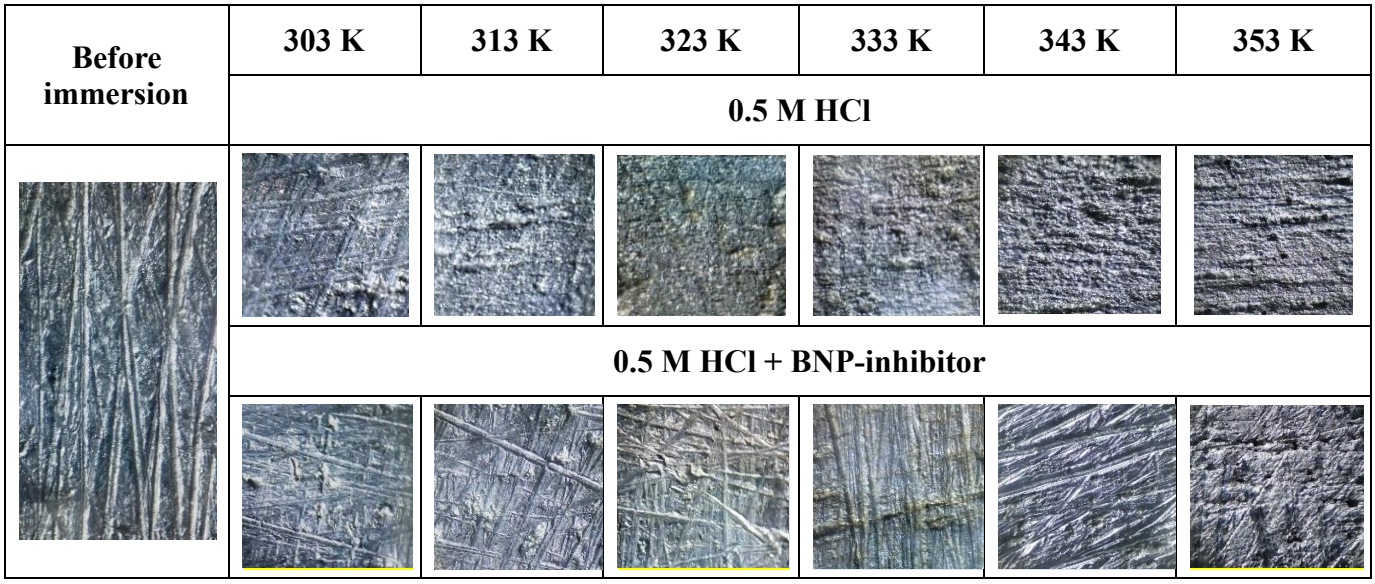

Figure 4. Microimages of the mild steel surface damage after 2 h immersion in 0.5 mol·dm^{-3} HCl with and without BNP-inhibitor containing H_3BO_3 + 1,4-PDA + Na_3PO_4 at the molar ratio of 3:2:1 ($\times10^{-3}$ mol·dm^{-3}) at different temperatures (×50).

The microscope image of the steel specimen indicates that the corrosion process is uniform across the metal surface. In the absence of the BNP-inhibitor, there is evidence of a uniformly dark and friable layer formation. Contrastingly, observations made after a 2-hour immersion time in the presence of the BNP-inhibitor reveal that the metal surface remains

bright, albeit losing its original lustre. Simultaneously, the metal's structure remains easily observable because the inhibitor has substantially reduced surface damage. The notable difference between steel surfaces with and without the BNP-inhibitor underscores the significant reduction in surface damage due to the robust protective effect of the BNP-inhibitor.

4. Conclusion

The purpose of the current study was to develop of effective corrosion inhibitor based on the combination of boron, nitrogen, and phosphorus compounds. Developed BNP-inhibitor containing H_3BO_3 ($3 \cdot 10^{-3}$ mol·dm^{-3}), 1,4-phenylenediamine ($2 \cdot 10^{-3}$ mol·dm^{-3}) and Na_3PO_4 ($1 \cdot 10^{-3}$ mol·dm^{-3}) demonstrate protective efficiency against corrosion of carbon steel in 0.5 mol·dm^{-3} HCl solution up to 93.2%. Due to the multi-component nature, the BNP-inhibitor is highly effective, easily *in situ* synthesised, and low cost. *In situ* formation of the inhibitor makes it possible to exclude synthetic and purification preliminary stages. The weight loss results demonstrated that the nature and molar ratio of components are crucial for inhibitor efficiency. The Langmuir model emerged as the most suitable for describing the adsorption of the developed inhibitor. Analysis of the data on free Gibbs energy and activation parameters allowed for the conclusion that the adsorption of the BNP-inhibitor on the carbon steel surface is a spontaneous and exothermic physisorption process.

References

1. R.W. Revie and H.H. Uhlig, *Corrosion and Corrosion Control: An Introduction to Corrosion Science and Engineering*, John Wiley & Sons Inc., New Jersey, USA, 2008, 490. doi: 10.1002/9780470277270
2. W. Zhao, F. Li, X. Lv, J. Chang, S. Shen, P. Dai, Y. Xia and Z. Cao, Research Progress of Organic Corrosion Inhibitors in Metal Corrosion Protection, *Crystals*, 2023, **13**, no. 9, 1329. doi: 10.3390/cryst13091329
3. A.A. Al-Amiery, W.N.R.W. Isahak and W.K. Al-Azzawi, Corrosion Inhibitors: Natural and Synthetic Organic Inhibitors, *Lubricants*, 2023, **11**, 174. doi: 10.3390/lubricants11040174
4. H. Jafari and K. Sayin, Sulfur Containing Compounds as Corrosion Inhibitors for Mild Steel in Hydrochloric Acid Solution, *Trans. Indian Inst. Met*., 2016, **69**, 805–815. doi: 10.1007/s12666-015-0556-2
5. M. Sahin, S. Bilgic and H. Yılmaz, The inhibition effects of some cyclic nitrogen compounds on the corrosion of the steel in NaCl mediums, *Appl. Surf. Sci*., 2002, **195**, no. 1–4, 1–7. doi: 10.1016/S0169-4332(01)00783-8
6. L. Liu, T. Cao, Q. Zhang and C. Cui, Organic Phosphorus Compounds as Inhibitors of Corrosion of Carbon Steel in Circulating Cooling Water: Weight Loss Method and Thermodynamic and Quantum Chemical Studies, *Adv. Mater. Sci. Eng*., 2018, 1653484. doi: 10.1155/2018/1653484

7. J. Cui, W. Yuan and Y. Pei, Corrosion resistance of carbon steel under an aerobic acidic condition in the presence of borate as corrosion inhibitor, *Anti-Corros. Methods Mater*., 2019, **66**, no. 1, 88–100. doi: 10.1108/ACMM-04-2018-1918
8. V.O. Izionworu, C.P. Ukpaka and E.E. Oguzie, Green and Eco-Benign Corrosion Inhibition Agents: Alternatives and Options to Chemical Based Toxic Corrosion Inhibitors*, Chem. Int*., 2020, **6**, no. 4, 232–259. doi: 10.5281/zenodo.3706592
9. Ya.G. Avdeev and Yu.I. Kuznetsov, Acid corrosion of metals and its inhibition. A critical review of the current problem state, *Int. J. Corros. Scale Inhib*., 2022, **11**, no. 1, 111–141. doi: 10.17675/2305-6894-2022-11-1-6
10. A. Thorn, A. Adams, T. Gichuhi, W. Novelli and M.A.S. Halox, Improved corrosion control through nontoxic corrosion inhibitor synergies, *JCT CoatingsTech*, 2006, **3**, no. 5, 24–30.
11. A.A. Al-Amiery, E. Yousif, W.N.R.W. Isahak and W.K. Al-Azzawi, A Review of Inorganic Corrosion Inhibitors: Types, Mechanisms, and Applications, *Tribol. Ind*., 2023, **45**, no. 2, 313–339. doi: 10.24874/ti.1456.03.23.06
12. F.U. Shah, Boron compounds as additives to lubricants: synthesis, characterization and tribological optimization, Licentiate dissertation, Luleå tekniska universitet, 2009, 61.
13. F.U. Shah, S. Glavatskih and O.N. Antzutkin, Boron in Tribology: From Borates to Ionic Liquids, *Tribol. Lett*., 2013, **51**, 281–301. doi: 10.1007/s11249-013-0181-3
14. E. Kir, B. Gurler and A. Gulec, Boron removal from aqueous solution by using plasma-modified and unmodified anion-exchange membranes, *Desalination*, 2011, **267**, no. 1, 114–117. doi: 10.1016/j.desal.2010.08.037
15. V. Aubakirova, R. Farrakhov, V. Astanin, A. Sharipov, M. Gorbatkov and E. Parfenov, Plasma Electrolytic Oxidation of Zr-1%Nb Alloy: Effect of Sodium Silicate and Boric Acid Addition to Calcium Acetate-Based Electrolyte, *Materials*, 2022, **15**, no. 6, 2003. doi: 10.3390/ma15062003
16. S.M. Gaidar, R.K. Nizamov, M.I. Golubev and I.G. Golubev, Protective Efficiency of Water-Soluble Corrosion Inhibitors, *Mordovia Univ. Bull*., 2018, **28**, no. 3, 429–444. doi: 10.15507/0236-2910.028.201803.429-444
17. J. Cui, Y. Yang, X. Li, W. Yuan and Y. Pei, Toward a Slow-Release Borate Inhibitor to Control Mild Steel Corrosion in Simulated Recirculating Water, *ACS Appl. Mater. Interfaces*, 2018, **10**, no. 4, 4183–4197. doi: 10.1021/acsami.7b15507
18. A. Elbadaoui, M. Galai, S. Ferraa, H. Barebita, M. Cherkaoui and T. Guedira, A new family of borated glasses as a corrosion inhibitor for steel in 1.0 M hydrochloric acid: synthesis and cauterization studies, *Int. J. Corros. Scale Inhib*., 2022, **11**, no. 2, 666–685. doi: 10.17675/2305-6894-2022-11-2-15
19. H. El Boulifi, M. Ouakki, H. Barebita, T. Guedira and M. Cherkaoui, Assessing the corrosion inhibition performance of two borate-based glasses for mild steel in hydrochloric acid, *Mater. Today Proc*., 2020, **37**, no. 3, 3967–3972. doi: 10.1016/j.matpr.2020.09.658

20. N.D. Nam, Q.V. Bui, M. Mathesh, M.Y.J. Tan and M. Forsyth, A study of 4-carboxyphenylboronic acid as a corrosion inhibitor for steel in carbon dioxide containing environments, *Corros. Sci*., 2013, **76**, 257–266. doi: 10.1016/j.corsci.2013.06.048
21. I. Zarina and R. Ignash, Boron-Coordinated Compounds with Polyols and Inhibitation of Metal Corrosion, *Sci. J. Riga Tech. Univ*., 2011, **23**, 34–37.
22. G. Gece and S. Bilgiç, A computational study of two hexitol borates as corrosion inhibitors for steel, *Int. J. Corros. Scale Inhib*., 2017, **6**, no. 4, 476–484. doi: 10.17675/2305-6894-2017-6-4-7
23. Ya.G. Avdeev and Yu.I. Kuznetsov, Nitrogen-containing five-membered heterocyclic compounds as corrosion inhibitors for metals in solutions of mineral acids – an overview, *Int. J. Corros. Scale Inhib*., 2021, **10**, no. 2, 480–540. doi: 10.17675/2305-6894-2020-10-2-2
24. Ya.G. Avdeev Nitrogen-containing six-membered heterocyclic compounds as corrosion inhibitors for metals in solutions of mineral acids – A review, *Int. J. Corros. Scale Inhib*., 2018, **7**, no. 4, 460–497. doi: 10.17675/2305-6894-2018-7-4-1
25. H. Wang, P. Zhang, G. Fei, Y. Ma, N. Rang and Y. Kang, Design and properties of environmental anticorrosion coating based on *m*-aminobenzenesulfonic acid/aniline/*p*-phenylenediamine terpolymer, *Prog. Org. Coat*., 2019, **137**, 105274. doi: 10.1016/j.porgcoat.2019.105274
26. J.-W. Zhang and Y. Li, Green synthesis of poly(o-phenylenediamine) polymer film on stainless steel as a corrosion protection layer, *J. Appl. Polym. Sci*., 2021, **139**, no. 5, 51572. doi: 10.1002/app.51572
27. K.J. Croes, A.J. Vreugdenhil, M. Yan, T.A. Singleton, S. Boraas and V.J. Gelling, An electrochemical study of corrosion protection by in situ oxidative polymerization in phenylenediamine crosslinked sol-gel hybrid coatings, *Electrochim. Acta*, 2011, **56**, no. 23, 7796–7804. doi: 10.1016/j.electacta.2011.06.046
28. R.T. Vashi and B.B. Patel, Effect of Orthophenylenediamine on the Corrosion Inhibition of Brass in Nitric Acid Solution, *Int. J. Innovative Res. Sci. Eng. Technol*., 2017, **6**, no. 10, 19623–19635. doi: 10.15680/IJIRSET.2017.0610069
29. J. Telegdi, History of phosphorus-containing corrosion inhibitors: From the beginning till the present time, *in Water-Formed Deposits Fundamentals and Mitigation Strategies*, Eds.: Z. Amjad and K.D. Demadis, Elsevier, 2022, 49–68. doi: 10.1016/B978-0-12-822896-8.00004-2
30. L. Yohai, W. Schreiner, M. Vázquez and M.B. Valcarce, Phosphate ions as effective inhibitors for carbon steel in carbonated solutions contaminated with chloride ions, *Electrochim. Acta*, 2016, **202**, 231–242. doi: 10.1016/j.electacta.2015.10.167
31. I.M. Zin, S.B. Lyon and V.I. Pokhmurskii, Corrosion control of galvanized steel using a phosphate/calcium ion inhibitor mixture, *Corros. Sci*., 2003, **45**, no. 4, 777–788. doi: 10.1016/S0010-938X(02)00130-0

32. D.M. Bastidas, U. Martin, J.M. Bastidas and J. Ress, Corrosion inhibition mechanism of steel reinforcements in mortar using soluble phosphates: A critical review, *Materials*, 2021, **14**, no. 20, 1–34. doi: 10.3390/ma14206168
33. A. Al-Borno, M. Islam and R. Haleem, Synergistic effects observed in nitrite-inorganic phosphate inhibitor blends, *Corrosion*, 1989, **45**, no. 12, 990–995. doi: 10.5006/1.3585018
34. X. Gao, S. Liu, H. Lu, F. Gao and H. Ma, Corrosion inhibition of iron in acidic solutions by monoalkyl phosphate esters with different chain lengths, *Ind. Eng. Chem. Res*., 2015, **54**, no. 7, 1941–1952. doi: 10.1021/ie503508h
35. Y. Liu and P. Zhang, Review of Phosphorus-Based Polymers for Mineral Scale and Corrosion Control in Oilfield, *Polymers*, 2022, **14**, no. 13, 2673. doi: 10.3390/polym14132673
36. L.K.M.O. Goni and M.A.J. Mazumder, *in Corrosion Inhibitors*, Ed.: A. Singh, IntechOpen, 2019, 1–18. doi: 10.5772/intechopen.81376
37. P. Mutombo and N. Hackerman, The effect of some organophosphorus compounds on the corrosion behaviour of iron in 6 M HCl, *Anti-Corros. Methods Mater*., 1998, **45**, no. 6, 413–418. doi: 10.1108/00035599810236559
38. S. Mukherjee and R.D. Gupta, Organophosphorus Nerve Agents: Types, Toxicity, and Treatments, *J. Toxicol*., 2020, 3007984. doi: 10.1155/2020/3007984
39. V.I. Levashova and I.V. Yangirova, Synthesis and Inhibitory Properties of Compositions Based on Boric Acid, Mixture of Individual Polyethylene Polyamines and Hexamethylenetetramine, *Pet. Chem*., 2016, **56**, 73–76. doi: 10.1134/S0965544115070099
40. A. Kalendová, D. Vesely, M. Kohl and J. Stejskal, Effect of surface treatment of pigment particles with polypyrrole and polyaniline phosphate on their corrosion inhibiting properties in organic coatings, *Prog. Org. Coat*., 2014, **77**, no. 9, 1465–1483. doi: 10.1016/j.porgcoat.2014.04.012
41. M.A.A. El-Ghaffar, N.A. Abdel-Wahab, M.A. Sanad and M.W. Sabaa, High performance anti-corrosive powder coatings based on phosphate pigments containing poly(*o*-aminophenol), *Prog. Org. Coat*., 2015, **78**, 42–48. doi: 10.1016/j.porgcoat.2014.09.021
42. M.A.A. El-Ghaffar, A.M. Baraka, M.M. Hefny, E.A. Youssef and M.M. Aly, Boron Phosphate/Poly(*p*-phenylenediamine) as a Corrosion Inhibitive System for Steel Protection, *Egypt. J. Chem*., 2018, **61**, 759–771. doi: 10.21608/ejchem.2018.4184.1373
43. ISO 8407-2021 Corrosion of metals and alloys – Removal of corrosion products from corrosion test specimens, Geneva, Switzerland, 2021.
44. L.E. Tsygankova, V.I. Vigdorovich, N.V. Shel and E.V. Dubinskaya, Peculiarities of protective efficiency of nitrogen containing inhibitors of steel corrosion, *Int. J. Corros. Scale Inhib*., 2013, **2**, no. 4, 304–310. doi: 10.17675/2305-6894-2013-2-4-304-310

45. N.V. Akatyev and T.B. Seilova, Investigation of anticorrosive properties of aqueous extracts from common knotgrass (*Polygonum aviculare* L.) growing in the territory of West Kazakhstan region, *Universum: Tech. Sci*., 2023, **113**, no. 8, 38–48 (in Russian). doi: 10.32743/unitech.2023.113.8.15865
46. O. Alaba, O. Johnson and E. Leke, Thermodynamics and adsorption study of the corrosion inhibition of mild steel by *Euphorbia heterophylla L*. extract in 1.5 M HCl, *Results Mater*., 2020, **5**, 100074. doi: 10.1016/j.rinma.2020.100074
47. F. Ojo, I. Adejoro, K. Akpomie, B. Ogunyemi and E. Oyeka, Effect of Iodide Ions on the Inhibitive Performance of O-, M-, P-Nitroaniline on Mild Steel in Hydrochloric Acid Solution, *J. Appl. Sci. Environ. Manage*., 2018, **22**, no. 5, 775–782. doi: 10.4314/jasem.v22i5.32
48. E.A. Noor, Temperature Effects on the Corrosion Inhibition of Mild Steel in Acidic Solutions by Aqueous Extract of Fenugreek Leaves, *Int. J. Electrochem. Sci*., 2007, **2**, no. 12, 996–1017. doi: 10.1016/S1452-3981(23)17129-X
49. A. Kadhim, A.A. Al-Amiery, R. Alazawi, M.K.S. Al-Ghezi and H. Abass, Corrosion inhibitors. A review, *Int. J. Corros. Scale Inhib*., 2021, **10**, no. 1, 54–67. doi: 10.17675/2305-6894-2021-10-1-3
50. M. Gong, C. Jiang, X. Zheng, X. Zeng, X. Lin, Corrosion Inhibition of Carbon Steel in Sulfuric Acid by [BMIm] [Lys] Amino Acid Ionic Liquids, *Adv. Mater. Res*., 2012, **476–478**, 1434–1440. doi: 10.4028/www.scientific.net/AMR.476-478.1434
51. O. Dagdag, Z. Safi, H. Rachid, H. Erramli, M. El Bouchti, N. Wazzan, L. Guo, C. Verma, E.E. Ebenso and A. El Harfi, Epoxy pre-polymers as new and effective materials for corrosion inhibition of carbon steel in acidic medium: Computational and experimental studies, *Sci. Rep*., 2019, **9**, 11715. doi: 10.1038/s41598-019-48284-0
52. A. Ali, S. Falih, N. Yousif, R. Rezgar and I. Kamal, Modeling and Optimization of Structural Steel Corrosion Inhibition using Barely Grass Extract as Green Inhibitor, *Am. J. Environ. Eng*., 2017, **7**, no. 4, 73–81. doi: 10.5923/j.ajee.20170704.01
53. H. Gerengi, K. Schaefer and H.I. Sahin, Corrosion-inhibiting effect of Mimosa extract on brass-MM55 corrosion in 0.5 M H_2SO_4 acidic media, *J. Ind. Eng. Chem*., 2012, **18**, no. 6, 2204–2210. doi: 10.1016/j.jiec.2012.06.019
54. M. Kilo, H.T. Rahal, M.H. El-Dakdouki and A.M. Abdel-Gaber, Study of the corrosion and inhibition mechanism for carbon steel and zinc alloys by an eco-friendly inhibitor in acidic solution, *Chem. Eng. Commun*., 2021, **208**, no. 12, 1676–1685. doi: 10.1080/00986445.2020.1811239
55. C. Verma, M.A. Quraishi, L.O. Olasunkanmi and E.E. Ebenso, L-Proline-promoted synthesis of 2-amino-4-arylquinoline-3-carbonitriles as sustainable corrosion inhibitors for mild steel in 1 M HCl: experimental and computational studies, *RSC Adv*., 2015, **5**, 85417–85430. doi: 10.1039/C5RA16982H
56. A. Yurt, S. Ulutas and H. Dal, Electrochemical and theoretical investigation on the corrosion of aluminium in acidic solution containing some Schiff bases, *Appl. Surf. Sci*., 2006, **253**, no. 2, 919–925. doi: 10.1016/j.apsusc.2006.01.026

57. H. Ashassi-Sorkhabi, M.R. Majidi and K. Seyyedi, Investigation of inhibition effect of some amino acids against steel corrosion in HCl solution, *Appl. Surf. Sci*., 2004, **225**, no. 1–4, 176–185. doi: 10.1016/j.apsusc.2003.10.007
58. S. Xiong, J. Si, J. Sun, H. Wu, H. Dong and C. Zhang, Experimental and computational studies on heterocyclic organic compounds as corrosion inhibitors for copper immersed in O/W emulsion medium, *Anti-Corros. Methods Mater*., 2020, **67**, no. 2, 214–227. doi: 10.1108/ACMM-10-2019-2200
59. J.M.D. Olivo, B. Brown and S. Nesic, Modeling of corrosion mechanisms in the presence of quaternary ammonium chloride and imidazoline corrosion inhibitors, *NACE Int. Corros. Conf. Ser*., 2016, **3**, 2060–2073.

♦ ♦ ♦